Proceedings of the 10th
World Congress on Intelligent Control and Automation
July 6-8, 2012, Beijing, China

Design and Mathematical Modeling of a 4-Standard-Propeller (4SP) Quadrotor

Swee King Phang, Chenxiao Cai, Ben M. Chen, Tong Heng Lee

***Abstract*— The recent development of small yet sophisticated sensors has led to the development of smaller unmanned aerial vehicles, especially in the form of quadrotor. When it is limited by the availability of the reverse propellers, the conventional quadrotor will no longer be realizable, and thus introducing the 4-standard-propeller (4SP) quadrotor design. This paper presents a comprehensive nonlinear modeling of a 4SP quadrotor, and the guidelines to design it. The advantages of constructing such aircraft and its detailed working principle are first highlighted. A nonlinear mathematical model is then derived based on the first-principles approach. The model parameters are finally identified and verified through actual flight tests.**

***Index Terms*— Micro aerial vehicle, quadrotor, nonlinear model, 4-standard-propeller quadrotor.**

I. Introduction

The development of unmanned aerial vehicles (UAV) has generated great interest in the automatic control area in the last few decades. Throughout the history the UAV has been an invisible player in military applications [1] and civilian applications [2], usually used for surveillance, border patrolling, mine detection, aerial delivery of payload, forest fires monitoring, environmental protection, film production, etc. Such vehicles have also received a growing interest from many academic research institutes due to its high application potential and research value [3][4][5].

As the technology advancement makes smaller yet smarter electronic components and actuators possible, researchers are shifting their attention towards the development of micro-aerial vehicles (MAV), which are generally miniaturized UAVs. A relatively new type of rotorcraft, the so-called quadrotor, has slowly became the main focus in realizing the MAV concepts due to its simplicity.

Similar to any rotorcrafts, quadrotor has the potential to takeoff, hover, fly, and land, but in a much constrained and smaller area. It has a simple control mechanism, where the main actuators are the four independent propellers attached at each corner of the aircraft body. For a standard quadrotor, it consists of a pair of propellers rotating in the counter clockwise direction (direction for standard propellers) and another pair in the reverse direction to produce zero net yaw torque. The afore-mentioned standard quadrotors have been the subject of significant study since gaining the attention of robotics researchers in the early 2000s. Numerous works has been documented concerning the quadrotor dynamics and the methods to regulate their flight [6].

Fig. 1. A 4-standard-propeller quadrotor

In the event where the clockwise spinning propeller, which is also known as the reverse or non-standard propeller, is unavailable, several researchers have introduced an effective solution by utilizing all four standard propeller, with two of the propellers installed slightly slanted off the quadrotor's frame [7]. This alternative is particularly useful when cost and dimension of the aircraft are the concerning factors, as smaller reverse propellers are usually either unavailable or rather expensive if specially manufactured. A quadrotor of such configuration is shown in Fig. 1.

It is found that the development of such 4-standard-propeller (4SP) quadrotor is, however, still immature in the market. There are no firm clarification on the design parameters of such aircraft, such as the optimal slanting angle of the propellers. In this paper, we wish to provide the readers a guideline in designing a 4SP quadrotor, with a fairly completed nonlinear model of such aircraft is derived. Ultimately, the optimal design parameter —slanting angle of the propellers will also be proposed.

The paper is organized as follows. Section II discusses the 4SP quadrotor design and its working principle. Section III presents the nonlinear dynamic modeling of the 4SP quadrotor, while Section IV illustrates an optimal propellers orientation design. Section V shows the parameters identification results and model verification through computer simulation. Finally, the major conclusions of the paper are drawn in Section VI.

S. K. Phang is with the NUS Graduate School for Integrative Sciences & Engineering (NGS), National University of Singapore (NUS), Singapore. E-mail: king@nus.edu.sg

C. Cai, B. M. Chen and T. H. Lee are with the Department of Electrical & Computer Engineering, National University of Singapore (NUS), Singapore. E-mail: {elecaic,bmchen,eleleeth}@nus.edu.sg

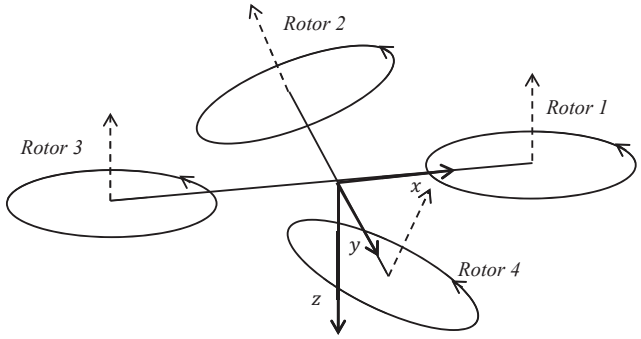

Fig. 2. Rotor number and body frame of 4SP quadrotor

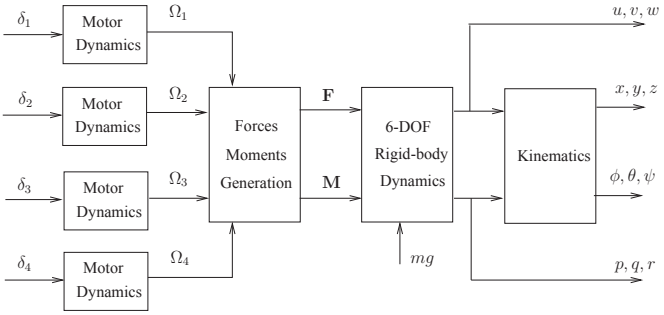

Fig. 4. Overview block diagram of the quadrotor model

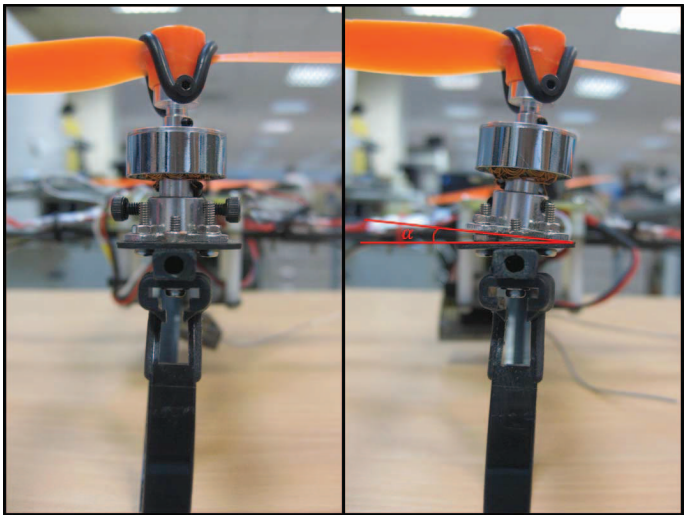

Fig. 3. **Left :** Rotor 1 & Rotor 3; **Right :** Rotor 2 & Rotor 4

II. 4SP Quadrotor Design and Working Principle

A 4SP quadrotor consists of four standard propeller systems in which all four of them spins at counter-clockwise direction, as shown in Fig. 2. Here, the rotor numbers $1, 2, 3$ and 4 correspond to the *front*, *left*, *back*, and *right* rotors. In order to maintain a zero net yaw moment (rotation around z-axis), propeller 2 and 4 are mounted slightly slanted along the x-axis at an angle of α (see Fig. 3). Note that the magnitude of the slanting angle, α, is the same for both propeller 2 and 4, but in the opposite direction. The optimal design value of α will be formulated in Section IV.

In hovering flight, the sum of rotational moments from each rotor will be completely canceled out by the moment due to the thrust components on x-axis of rotor 2 and rotor 4. While pitching or rolling, two opposite rotor will change their rotating speed, with one increase and another decrease, to create a non-zero net moment along the axes. As for yaw angle movement, rotor 1 and rotor 3 will increase (decrease) while rotor 2 and rotor 4 decrease (increase) to create yaw moment. By adapting the value of α which will be discussed later, one can assure that the four main movements — rolling, pitching, yawing, and heave movement will be completely independent of each other. In other words, the 4SP quadrotor can be controlled similar to the convention quadrotor.

III. Nonlinear Modeling of 4SP Quadrotor

A model overview block diagram of the 4SP quadrotor is presented in Fig. 4. Note that the outputs are displayed on the right of each block, while the inputs are shown on the left. Common symbols and variables to be used in the derivation are listed in Table I.

Symbols	Descriptions
$\mathbf{P_n}$	Position vector in NED frame $\equiv \begin{bmatrix} x & y & z \end{bmatrix}^T$
$\mathbf{V_b}$	Velocity vector in body frame $\equiv \begin{bmatrix} u & v & w \end{bmatrix}^T$
$\mathbf{\Theta}$	Euler angles $\equiv \begin{bmatrix} \phi & \theta & \psi \end{bmatrix}^T$
ω	Angular velocity $\equiv \begin{bmatrix} p & q & r \end{bmatrix}^T$
A	Area swipe by rotating propeller
C_T	Aerodynamic thrust coefficient
C_Q	Aerodynamic moment coefficient
δ_n	Input to the n-th motor
G	Gear ratio of motor to propeller
g	Gravitational force
J_{XX}	Moment of inertia along x-axis
J_{YY}	Moment of inertia along y-axis
J_{ZZ}	Moment of inertia along z-axis
J_p	Moment of inertia of single propeller
k_T	Thrust constant
k_Q	Moment constant
k_i	Current constant of motor
k_m	Motor dynamics DC gain
k_v	Voltage constant of motor
l	Length of a single quadrotor's arm
m	Mass of aircraft
ω_m	Natural frequency of motor dynamic
Ω_n	n-th propeller rotation rate
Q_n	Torque produced by the n-th propeller
$Q_{m,n}$	Torque of n-th motor
R	Motor resistance
r	Radius of the propeller
ρ	Air density
T_n	Thrust produced by the n-th propeller
V_n	Voltage input to the n-th motor
ζ_m	Damping ratio of motor dynamic

TABLE I

Descriptions of common symbols in the model

A few assumptions are made in deriving the model:

1) The origin of the body frame is coincident with the Center of Gravity (CG) of the 4SP quadrotor;
2) Axes of body frame coincide with body principal axes of inertia, i.e. the moment of inertia of aircraft body, $\mathbf{J}$, is diagonal;
3) Propellers are assumed rigid due to its small size, i.e. no blade flapping occurs.

A. Coordinate Systems

As a common practice of aeronautic analysis, two main coordinate frames will be used in the derivation. One is the North-East-Down (NED) frame and the other is the body frame. The NED frame is stationary with respect to a static observer on the ground, where axes point towards the North, East and downwards direction. The body frame is placed at the Center of Gravity (CG) of the quadrotor helicopter, where its origin and orientation move together with the helicopter fuselage. It is important to note that the x-axis pointed to the front of the aircraft, the y-axis to the right of the aircraft, and the z-axis pointed downwards in body frame (see Fig. 2).

The equations of motion are more conveniently formulated in the body frame for a few reasons [8]:

1) The inertia matrix is time-invariant;
2) Quadrotor body symmetry can greatly simplify the equations;
3) Measurement obtained onboard are mostly given in body frame, or can be easily converted to body frame;
4) Control forces are almost always given in body frame.

B. Kinematics

To obtain the translational and rotational motions between the NED and the body coordinate systems, one has the following well-known navigation equations [9][10]:

$$\dot{\mathbf{P}}_\mathbf{n} = \mathbf{R}_{\mathbf{n/b}}\mathbf{V_b}, \quad (1)$$

$$\dot{\mathbf{\Theta}} = \mathbf{S}^{-1}\omega, \quad (2)$$

where the rotational matrix, $\mathbf{R_{n/b}}$, and the lumped transformation matrix, $\mathbf{S}^{-1}$ are given by

$$\mathbf{R_{n/b}} = \begin{bmatrix} c_\theta c_\psi & s_\phi s_\theta c_\psi - c_\phi s_\psi & c_\phi s_\theta c_\psi + s_\phi s_\psi \\ c_\theta s_\psi & s_\phi s_\theta s_\psi + c_\phi c_\psi & c_\phi s_\theta s_\psi - s_\phi c_\psi \\ -s_\theta & s_\phi c_\theta & c_\phi c_\theta \end{bmatrix}, \quad (3)$$

$$\mathbf{S}^{-1} = \begin{bmatrix} 1 & s_\phi t_\theta & c_\phi t_\theta \\ 0 & c_\phi & -s_\phi \\ 0 & s_\phi/c_\theta & c_\phi/c_\theta \end{bmatrix}, \quad (4)$$

with $s_* = \sin(*)$, $c_* = \cos(*)$, and $t_* = \tan(*)$.

Note that the rotational matrix, $\mathbf{R_{n/b}}$, is orthogonal, thus its inverse is identical to its transpose, i.e., $\mathbf{R_{n/b}}^{-1} = \mathbf{R_{n/b}}^{T}$.

C. 6 Degree-of-Freedom Rigid Body Dynamics

By using the Newton-Euler formalism which describe the translational and rotational dynamics of a rigid-body, the following two dynamics equations take into account of the mass of the aircraft, m, and its inertia matrix, $\mathbf{J}$.

$$m\dot{\mathbf{V}}_\mathbf{b} + \omega \times (m\mathbf{V_b}) = \mathbf{F}, \quad (5)$$

$$\mathbf{J}\dot{\omega} + \omega \times (\mathbf{J}\omega) = \mathbf{M}, \quad (6)$$

where $\mathbf{F}$ and $\mathbf{M}$ are the force and moment vectors acting on the body. As mentioned in the previous section, the inertia matrix, $\mathbf{J}$, is diagonal, i.e.,

$$\mathbf{J} = \begin{bmatrix} J_{XX} & 0 & 0 \\ 0 & J_{YY} & 0 \\ 0 & 0 & J_{ZZ} \end{bmatrix}. \quad (7)$$

D. Forces and Moments Generation

According to [8] and [11], the force and torque vectors are contributed by four major sources. More specifically, they are the gravitational force, the main movement inputs produced by spinning rotors, its reaction torques, and the gyroscopic effects. The gravitational force only affect the linear movement of the quadrotor, while the reaction torques and gyroscopic moments affect only the angular movement of the aircraft. As a result, the force and moment vectors are divided into these parts, i.e.,

$$\begin{bmatrix} \mathbf{F} \\ \mathbf{M} \end{bmatrix} = \begin{bmatrix} \mathbf{F_{gravity}} \\ \mathbf{0} \end{bmatrix} + \begin{bmatrix} \mathbf{F_{rotor}} \\ \mathbf{M_{rotor}} \end{bmatrix} + \begin{bmatrix} \mathbf{0} \\ \mathbf{M_{reaction}} \end{bmatrix} + \begin{bmatrix} \mathbf{0} \\ \mathbf{M_{gyro}} \end{bmatrix}. \quad (8)$$

1) Gravitational Force: The first component is the gravitational force vector $\mathbf{F_{gravity}}$ given from the acceleration due to gravity, g. As the gravitational force acts only on the z-axis of the NED frame, by transforming it to the body frame, we have

$$\mathbf{F_{gravity}} = \mathbf{R_{n/b}}^{-1} \begin{bmatrix} 0 \\ 0 \\ mg \end{bmatrix} = \begin{bmatrix} -mgs_\theta \\ mgc_\theta s_\phi \\ mgc_\theta c_\phi \end{bmatrix}. \quad (9)$$

2) Rotor Movements: The forces and torques directly produced by the rotor movements contributed to most of the forces and moments generated. For each of the rotating rotor, it creates a thrust, T_n, and a torque, Q_n, for $n = 1, 2, 3, 4$ along its axis. From the aerodynamics consideration, the thrust and torques created can be represented as

$$T_n = C_T \rho A r^2 \Omega_n^2, \quad (10)$$

$$Q_n = C_Q \rho A r^3 \Omega_n^2, \quad (11)$$

where C_T and C_Q are the aerodynamic coefficients of the propeller, ρ is the density of the air, A and r are the disc area swept by the rotating rotor and the radius of the rotor blade. Since the aerodynamic coefficients is almost constant for small propellers, the equations can be simplified to

$$T_n = k_T \Omega_n^2, \quad (12)$$

$$Q_n = k_Q \Omega_n^2, \quad (13)$$

where k_T and k_Q can be obtained easily through some experiments.

Differing from the conventional quadrotor, the total thrust of the 4SP quadrotor is formulated as the summation of the thrust components in z-direction of each rotor. More specifically,

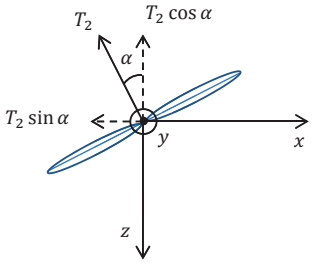

Fig. 5. Thrust decomposition for rotor 2 along x- and z-axis

since rotor 2 and rotor 4 are installed slanted towards the positive and negative x-direction (see Fig. 5), we have

$$\mathbf{F_{rotor}} = \begin{bmatrix} -s_\alpha T_2 + s_\alpha T_4 \\ 0 \\ -(T_1 + c_\alpha T_2 + T_3 + c_\alpha T_4) \end{bmatrix}. \quad (14)$$

Next, pitch and roll moments will be generated by the component thrust difference of the opposing rotors, with roll moments consist also the component moments by rotor 2 and rotor 4 at x-axis, while the yaw moments is generated based on the total component moments of each rotors at z-axis. The moment vector will then be

$$\mathbf{M_{rotor}} = \begin{bmatrix} c_\alpha l(T_2 - T_4) + s_\alpha(Q_2 - Q_4) \\ l(T_1 - T_3) \\ Q_1 + Q_3 + c_\alpha(Q_2 + Q_4) - s_\alpha l(T_2 + T_4) \end{bmatrix}. \quad (15)$$

Note that in the final equation, thrust T_n and moments Q_n should be written as $k_T\Omega_n^2$ and $k_Q\Omega_n^2$ respectively. Here they are left in this form due to space constraint.

3) Reaction Torques: Inertia counter torque, which is the reaction torque produced by the change in rotational speed of the rotor, is modeled as

$$\mathbf{M_{reaction}} = \begin{bmatrix} -J_p(s_\alpha\dot{\Omega}_2 - s_\alpha\dot{\Omega}_4) \\ 0 \\ -J_p(\dot{\Omega}_1 + \dot{\Omega}_3 + c_\alpha\dot{\Omega}_2 + c_\alpha\dot{\Omega}_4) \end{bmatrix}. \quad (16)$$

4) Gyroscopic Effects: Gyroscopic moments, caused by the combination of rotations of four propellers and the aircraft's body is commonly modeled in [12] and [13] as

$$\mathbf{M_{gyro}} = \sum_{k=1}^{4} J_p \left(\omega \times \begin{bmatrix} 0 \\ 0 \\ 1 \end{bmatrix} \right) (-1)^k \Omega_k, \quad (17)$$

where J_p is the total rotational moment of inertia around the propeller axis. Notice that, however, there are 2 major differences in the formulation between the conventional quadrotor with the 4SP quadrotor. First, all propeller in the 4SP quadrotor has the same counter-clockwise rotation. Second, two of the rotors (rotor 2 and rotor 4) are installed slanted at α degree.

Here, we adopt a more general form of gyroscopic moment generation, which is in the form of

$$\mathbf{M_{gyro,n}} = J_p(\omega \times \mathbf{r}_n)\Omega_n, \quad (18)$$

where $\mathbf{r}_n$ is the unit vector pointed at the rotational axis of the n-th propeller in body frame. As a result, the gyroscopic moments generated can be separated into 4 individual moments, as shown below:

$$\begin{aligned}
\mathbf{M_{gyro,1}} &= J_p \left(\omega \times \begin{bmatrix} 0 \\ 0 \\ -1 \end{bmatrix} \right) \Omega_1, \\
\mathbf{M_{gyro,2}} &= J_p \left(\omega \times \begin{bmatrix} -s_\alpha \\ 0 \\ -c_\alpha \end{bmatrix} \right) \Omega_2, \\
\mathbf{M_{gyro,3}} &= J_p \left(\omega \times \begin{bmatrix} 0 \\ 0 \\ -1 \end{bmatrix} \right) \Omega_3, \\
\mathbf{M_{gyro,4}} &= J_p \left(\omega \times \begin{bmatrix} s_\alpha \\ 0 \\ -c_\alpha \end{bmatrix} \right) \Omega_4.
\end{aligned}$$

The total gyroscopic moments will then be the summation of all 4 moments shown above, and thus its final form is given by

$$\mathbf{M_{gyro}} = \begin{bmatrix} J_p(-q\Omega_1 - c_\alpha q\Omega_2 - q\Omega_3 - c_\alpha q\Omega_4) \\ J_p(p\Omega_1 + (c_\alpha p - s_\alpha r)\Omega_2 + p\Omega_3 + (c_\alpha p + s_\alpha r)\Omega_4) \\ J_p(s_\alpha q\Omega_2 - s_\alpha q\Omega_4) \end{bmatrix}. \quad (19)$$

E. Motor Dynamics

A standard DC motor with negligible inductance is commonly modeled in [14] as

$$Q_{m,n} = k_i\left(V_n - \frac{k_v\Omega_n}{G}\right)/R, \quad (20)$$

$$\dot{\Omega}_n = \frac{GQ_{m,n} - Q_n}{J_p}. \quad (21)$$

To simplify the model for the ease of parameter identification, the motor dynamics can be written as a general second order system, i.e.,

$$\frac{\Omega_n}{\delta_n} = \frac{k_m\omega_m^2}{s^2 + 2\zeta_m\omega_m + \omega_m^2}. \quad (22)$$

Noted that in Equation (22), δ_n is the normalized input to the motor speed controller, with the following normalization process,

$$\delta_n = \frac{u_n - 1100}{840}, \quad (23)$$

where u_n is the pulse width fed to the motor speed controller in unit ms. In general, the minimum and maximum possible pulse width to the motor speed controller is at 1100 ms and 1940 ms respectively.

IV. Optimal Propellers Orientation Design

As observed from the mathematical model derived in the previous section, it is unclear if the movements are coupled. For example, one might question if the roll input movement induces yaw movement as there are 2 off-plane rotors. To solve the movement coupling problem, we present in this

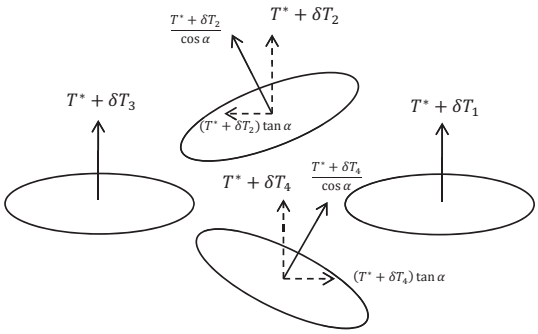

Fig. 6. Thrust produced by each rotor

paper a guideline to design the slanting angle (α) for rotor 2 and rotor 4 such that the four major input movements to the aircraft are completely decoupled.

Theorem 4.1 : In the 4SP quadrotor design, by assigning the slanting angle for rotor 2 and rotor 4 as

$$\alpha = \tan^{-1}\frac{2k_Q}{lk_T}, \tag{24}$$

then the four major input movements to the aircraft (rolling, pitching, yawing, and heave movement) will be completely decoupled.

Proof : As in Fig. 6, T^* is the equilibrium value of the thrust from each rotor to maintain hovering flight, with zero roll, pitch, yaw, and heave movement. Notice that the trim value T^* from rotor 2 and rotor 4 are the thrust component along z-axis, and thus the real thrusts produced by the two rotors are given by T^*/c_α, which are slightly larger. Notice also that the relationship between the thrust produced, T^*, and the moment produced, Q^*, is given by a linear factor k_T/k_Q. Therefore for a rotating rotor producing a thrust of T^*+t, it will produce a moment of Q^*+q where $T^*/Q^* = t/q = k_T/k_Q$ holds.

One can verify easily that at hovering flight, i.e. $\{\delta T_1, \delta T_2, \delta T_3, \delta T_4\} = \{0,0,0,0\}$, net moments on the aircraft body is

$$\begin{bmatrix} M_x \\ M_y \\ M_z \end{bmatrix} = \begin{bmatrix} Q^*t_\alpha - Q^*t_\alpha \\ 0 \\ 4Q^* - 2T^*lt_\alpha \end{bmatrix} = \begin{bmatrix} 0 \\ 0 \\ 4Q^* - 2T^*lt_\alpha \end{bmatrix}.$$

Thus by substituting $\tan\alpha = 2k_Q/lk_T$, the moments on the aircraft body will be

$$\begin{bmatrix} M_x \\ M_y \\ M_z \end{bmatrix} = \begin{bmatrix} 0 \\ 0 \\ 4Q^* - 2T^*l(2k_Q/lk_T) \end{bmatrix} = \mathbf{0},$$

which says that the quadrotor will stay stationary.

Similarly, in the translational heave movement when $\{\delta T_1, \delta T_2, \delta T_3, \delta T_4\} = \{t,t,t,t\}$, the moments vector is in the same form as the one in hovering flight. Replacing T^* and Q^* by T^*+t and Q^*+q, it is also resulting in zero net moments, showing that the aircraft will only translate along the z-axis.

For yaw input movement, i.e. $\{\delta T_1, \delta T_2, \delta T_3, \delta T_4\} = \{t,-t,t,-t\}$, the aircraft will have a zero heave movement as the additional thrusts t and $-t$ canceling one another. The moment vector will be

$$\begin{bmatrix} M_x \\ M_y \\ M_z \end{bmatrix} = \begin{bmatrix} (Q^*-q)t_\alpha - (Q^*-q)t_\alpha \\ 0 \\ 4Q^* - 2(T^*-t)lt_\alpha \end{bmatrix} = \begin{bmatrix} 0 \\ 0 \\ 4q \end{bmatrix},$$

which shows a pure yaw rotation.

As for pitch input movement, $\{\delta T_1, \delta T_2, \delta T_3, \delta T_4\} = \{t,0,-t,0\}$. Again, heave direction will have zero net movement, and the moment vector can be formulated as

$$\begin{bmatrix} M_x \\ M_y \\ M_z \end{bmatrix} = \begin{bmatrix} Q^*t_\alpha - Q^*t_\alpha \\ l(T^*+t) - l(T^*-t) \\ 4Q^* - 2(T^*)lt_\alpha \end{bmatrix} = \begin{bmatrix} 0 \\ 2lt \\ 0 \end{bmatrix},$$

which is a pure pitch rotation.

Finally, we have the roll input movement, i.e. $\{\delta T_1, \delta T_2, \delta T_3, \delta T_4\} = \{0,t,0,-t\}$. Similar to the pitch movement, the heave direction will have zero net movement. The moment vector is formulated as

$$\begin{aligned} \begin{bmatrix} M_x \\ M_y \\ M_z \end{bmatrix} &= \begin{bmatrix} (Q^*+q)t_\alpha - (Q^*-q)t_\alpha + l[(T^*+t)-(T^*-t)] \\ 0 \\ 4Q^* - [(T^*+t)+(T^*-t)]lt_\alpha \end{bmatrix} \\ &= \begin{bmatrix} 2qt_\alpha + 2lt \\ 0 \\ 0 \end{bmatrix}, \end{aligned}$$

which is a pure rolling movement.

It can be seen from the above derivation that by designing $\alpha = \tan^{-1} 2k_Q/lk_T$, the roll, pitch, yaw and heave movements of the aircraft are totally decoupled and hence can be controlled like a conventional quadrotor.

V. Parameter Identification and Model Verification Results

Several parameters in the model need to be identified, either by measurements or estimated experimentally. The main content of this paper is not on the parameter identification methods, and thus they are only briefly described here:

1) m, l can be measured directly;
2) J_{XX}, J_{YY}, J_{ZZ} can be obtained through the trifilar pendulum method introduced in [15];
3) k_m, ω_m, ζ_m can be estimated from test bench experiments;
4) k_T, k_Q can be obtained by plotting the thrust and torque produced against rotation speed of rotor;
5) J_p can be calculated Mathematically by approximating the propeller as a rectangular shape.

A. Verification Results

The identified parameters are shown in Table II. In order to evaluate on the fidelity of the obtained mathematical model, two flight tests were carried out by injecting sinusoidal input signal to the opposing rotors (first rotor 1 & rotor 3, then

Parameter	Value	unit
g	9.781	ms^{-2}
J_{XX}	1.0574×10^{-3}	kgm^2
J_{YY}	1.0574×10^{-3}	kgm^2
J_{ZZ}	2.4234×10^{-3}	kgm^2
J_p	3.1771×10^{-6}	kgm^2
k_T	1.294×10^{-6}	Ns^2
k_Q	1.095×10^{-8}	Nms^2
k_m	524.1667	
l	0.1675	m
m	0.235	kg
ω_m	40	rad/s
ζ_m	0.6	

TABLE II

PARAMETER IDENTIFIED

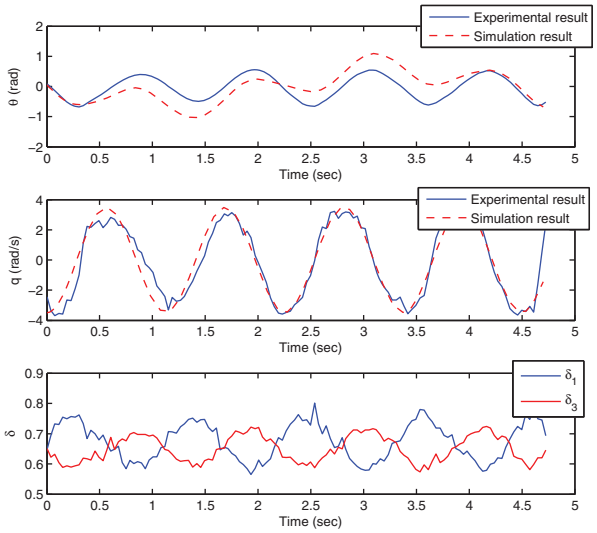

Fig. 7. Responses from pitch angle perturbation

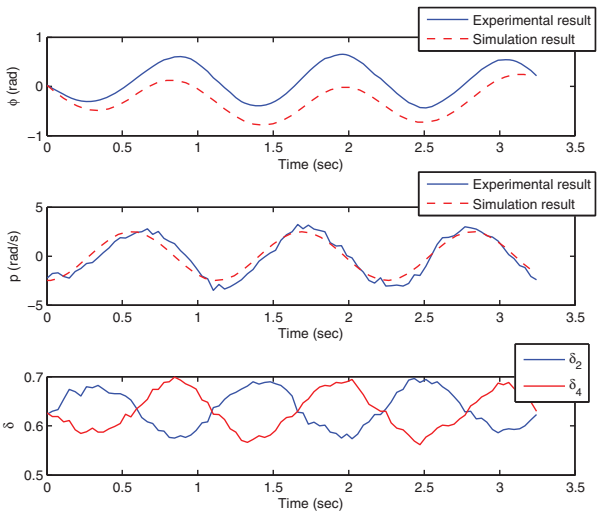

Fig. 8. Responses from roll angle perturbation

rotor 2 & rotor 4) to obtain the pitch and roll responses of the 4SP quadrotor. Figs. 7 and 8 show the time response of the pitch/roll angles and angular rates, together with the normalized input signal, δ_n. Note that the dotted lines are the simulation results calculated by MATLAB using the nonlinear model derived in the previous sections, while the solid lines are the measurements by the onboard sensors. The results has shown that the derived nonlinear mathematical model matches the real model, up to a rather high degree of accuracy, within the frequency range of interest (approx. 1 Hz).

VI. CONCLUSION

In this paper, the design and mathematical modeling of a 4SP quadrotor is discussed. Such 4SP configuration will be a good solution for quadrotor design when its dimension and cost are the main constrains. The working principle of the 4SP quadrotor is analyzed and a nonlinear model of the quadrotor is derived and formulated. Lastly, an optimal propellers orientation design is proposed to decouple the main input movements of the aircraft, which are respectively the rolling, pitching, yawing, and heave movements. One of such 4SP configuration quadrotor has been realized, and a few flight tests has been carried out to verify the finding.

REFERENCES

[1] B. Samir, M. Pierpaolo and S. Roland, "Towards Autonomous Indoor Micro VTOL," *Autonomous Robots,* 2005, vol. 18, no. 2, pp. 171–183.

[2] R. Sugiura, T. Fukagawa and N. Noguchi, "Field Information System Using an Agricultural Helicopter towards Precision Farming," *IEEE/ASME International Conference on Advanced Intelligent Mechatronics,* 2003, pp. 1073–1078.

[3] N. Kundak and B. Mettler, "Experimental Framework for Evaluating Autonomous Guidance and Control Algorithms for Agile Aerial Vehicles," *European Control Conference,* 2007, pp. 293–300.

[4] M. Valenti, B. Bethke, G. Fiore, J. P. How and E. Feron, "Indoor Multi-Vehicle Flight Testbed for Fault Detection, Isolation, and Recovery," *AIAA Guidance, Navigation and Control Conference and Exhibit,* 2006.

[5] S. L. Waslander, G. M. Hoffman, J. S. Jang and C. J. Tomlin, "Multi-Agent Quadrotor Testbed Control Design: Integral Sliding Mode vs. Reinforcement Learning," *IEEE/RSJ International Conference on Intelligent Robots and Systems,* 2005, pp. 3712–3717.

[6] P. Pounds, R. Mahony and P. Corke, "Modelling and Control of a Large Quadrotor Robot," *Control Engineering Practice,* 2010, vol. 18, pp 691–699.

[7] J. Julio, "ArduIMU Quadrotor Part II (mini)," Available Online: http://www.diydrones.com/profiles/blogs/arduimu-quadcopter-part-ii, 2010

[8] T. Bresciani, "Modelling, Identification and Control of a Quadrotor Helicopter," Master thesis, Lund University, Lund, Sweden, Oct, 2008.

[9] G. V. Raffo, M. G. Ortega and F. R. Rubio, "An Integral Predictive/Nonlinear H_∞ Control Structure for a Quadrotor Helicopter," *Automatica,* 2010, vol. 46, pp. 29–39.

[10] G. Cai, B. M. Chen and T. H. Lee, *Unmanned Rotorcraft Systems*, Springer, 2011.

[11] R. Goel, S. M. Shah, N. K. Gupta and N. Ananthkrishnan, "Modeling, Simulation and Flight Testing of an Autonomous Quadrotor," *Proceedings of International Conference on Environmental and Agriculture Engineering*, 2009.

[12] S. Bouabdallah, A. Noth and R. Siegwart, "PID vs LQ Control Techniques Applied to an Indoor Micro Quadrotor," *IEEE International Conference on Intelligent Robots and Systems,* 2004, pp. 2451–2456.

[13] T. Hamel, R. Mahony, R. Lozano and J. Ostrowski, "Dynamic Modelling and Configuration Stabilization for an X4-Flyer," *IFAC Triennial World Congress,* 2002.

[14] S. Bouabdallah, P. Murrieri and R. Siegwart, "Design and Control of an Indoor Micro Quadrotor," *IEEE International Conference on Robotics and Automation,* 2004, vol. 5, pp 4393–4398.

[15] C. M. Harris, Shock and Vibration Handbook , 4th ed. New York, NY:McGraw-Hill, 1996.